4.1 The numerical model and the control run

Though the OGCM simulations compare well with the observations, the OGCM is too complex to yield insight into the dynamics underlying the monsoon-current system. To isolate the processes responsible for forcing the monsoon currents, we need a model that has only the minimum physics required for simulating the wind-forced circulation in the upper ocean. For this, we use a dynamical $1\frac{1}{2}$-layer reduced-gravity model, in which the density of the model layers does not vary in space or time. The active upper layer is much shallower than the infinitely deep, motionless, lower layer. The equations for the upper layer are (Shankar, 1998)

$$(H\mathbf{v})_t + \nabla\cdot(\mathbf{v}H\mathbf{v}) + f\mathbf{k}\times(H\mathbf{v}) + g\overline{\Gamma}H\nabla H = \tau/\rho_1 + \nu\nabla^2(H\mathbf{v}) - \chi\mathbf{i}\cdot(H\mathbf{v}), \quad \text{(2a)}$$

$$H_t + \nabla\cdot(H\mathbf{v}) = \kappa\nabla^2 H, \quad \text{(2b)}$$

$$\eta = \overline{\Gamma}\left(H - \overline{H}\right), \quad \text{(2c)}$$

where $H = \overline{H} + h$ is the instantaneous layer thickness, $\overline{H}$ the initial layer thickness, h the deviation of the layer thickness from the initial value, $\mathbf{v} = (u, v)$ the velocity, $f = \beta y$ the Coriolis parameter, $\tau = (\tau^x, \tau^y)$ the wind stress, g the acceleration due to gravity, and $\overline{\Gamma} = \Delta\rho/\overline{\rho}$ the reduced-gravity parameter; $\Delta\rho = \rho_2 - \rho_1$, and $\overline{\rho}$ is an average density that is representative of the ocean; ν and κ are the Laplacian mixing coefficients for momentum and thickness, the latter being included to damp the small-scale noise in the H field, and χ is a Rayleigh friction coefficient; η is the deviation of model dynamic height, computed with respect to the motionless deep ocean, from the initial state. In the discussion that follows, we refer to η as the model sea level rather than as dynamic height. The model parameters are listed in Table 5.

Eqns. (2) are integrated numerically on an Arakawa C-grid using the leapfrog scheme; diffusive terms are evaluated at the backward time level and all other terms at the central time level. To inhibit time-splitting instability, the fields are averaged

between successive time levels every 41 time steps. The model domain is as in McCreary et al. (1993). The upper-layer thickness is not allowed to shallow beyond 10 m, or deepen beyond 190 m. The no-slip condition is applied at continental boundaries and the zero-gradient condition is applied at the open southern boundary at 29°S. A linear damper (Rayleigh friction) is applied on the zonal velocity field near the southern boundary; it is required to inhibit the development of large-scale instability along the boundary caused by the application of the zero-gradient condition on u. The damper is present only near the boundary, with $\chi = 1$ day^{-1}

Parameter (units)	Symbol	Value
Laplacian mixing coefficient for momentum (cm^2 s^{-1})	ν	5×10^7
Laplacian mixing coefficient for thickness (cm^2 s^{-1})	κ	1×10^7
Thermal expansion coefficient (°C^{-1})	α_T	-0.00025
Haline contraction coefficient (PSU^{-1})	α_S	0.00125
Reduced-gravity parameter	$\overline{\Gamma}$	0.0035
Initial upper layer thickness (m)	$\overline{H}$	100
Minimum upper layer thickness (m)	$H_{\min}$	10
Maximum upper layer thickness (m)	$H_{\max}$	190
Linear Kelvin wave speed for $\overline{H} = 100$ m (cm s^{-1})	c	185
Rossby wave speed at 10°N (cm s^{-1})	c_R	12.2
Grid size (km)	$\Delta x, \Delta y$	55
Time step (minutes)	Δt	72

Table 5
Parameters for the reduced-gravity model.

within 150 km of the boundary, and decreasing linearly to zero in the interval from 150 km to 300 km. There is no corresponding damper on v and H, so that fluid can pass freely through the boundary.

The forcing is derived from the wind-stress climatology of Hellerman and Rosenstein (1983) (Fig. 1), their wind stress being interpolated linearly to the model grid and then smoothed (McCreary et al., 1993; Shankar and Shetye, 1997). The model is spun up from a state of rest, the winds being ramped up from zero to the appropriate level over five days to damp inertial oscillations. Results discussed below are from the tenth year of the simulation, by when the solution approaches stationarity.

The solution (Fig. 16) emphasizes the geostrophic contribution to the flow. The contribution of the Ekman drift is weak, except in the western Arabian Sea, because the currents are averaged over the model upper layer. Westward propagation of sea-level anomalies is evident in the solution, especially in the eastern Bay of Bengal and southeastern Arabian Sea (Fig. 17). This solution compares well with the DAF of the OGCM (Fig. 12), except that the recirculation in the eddies off Somalia does not cross the equator, the eastward flow in the western equatorial Indian Ocean instead feeding the SMC south of Sri Lanka, as in the simulations of McCreary et al. (1993). The observations are also not clear in this regard, there being differences between the flow in the ship drifts (Fig. 9) and surface drifters (Shenoi et al., 1999a). Though there is less detail in the solution compared to the geostrophic flow estimated from TOPEX/Poseidon altimetry (Fig. 5), the model does capture the essential features of the monsoon currents on the seasonal time scale.

To examine to what extent these are attributable to nonlinear effects, we linearize the model equations to obtain (Shankar, 1998)

$$\mathbf{v}_t + f\mathbf{k}\times\mathbf{v} + g\overline{\Gamma}\nabla h = \frac{\tau}{\rho_1 \overline{H}} + \nu\nabla^2\mathbf{v} - \chi\mathbf{i}\cdot\mathbf{v}, \tag{3a}$$

$$h_t + \nabla\cdot\mathbf{v} = \kappa\nabla^2 h, \tag{3b}$$

$$\eta = \overline{\Gamma} h. \tag{3c}$$

The solution to these linear equations (Fig. 18) reproduces all the features seen in

the nonlinear simulation; the one major exception is the Great Whirl off Somalia, which owes its existence to nonlinear dynamics (Shankar and Shetye, 1997) and appears in the linear solution as part of a large anticyclonic gyre in the western Arabian Sea. Notwithstanding this discrepancy, the linear solution shows the strong poleward Somali Current, its recirculation in the gyres offshore, and the continuity of this current across the Arabian Sea to the southern tip of Sri Lanka.

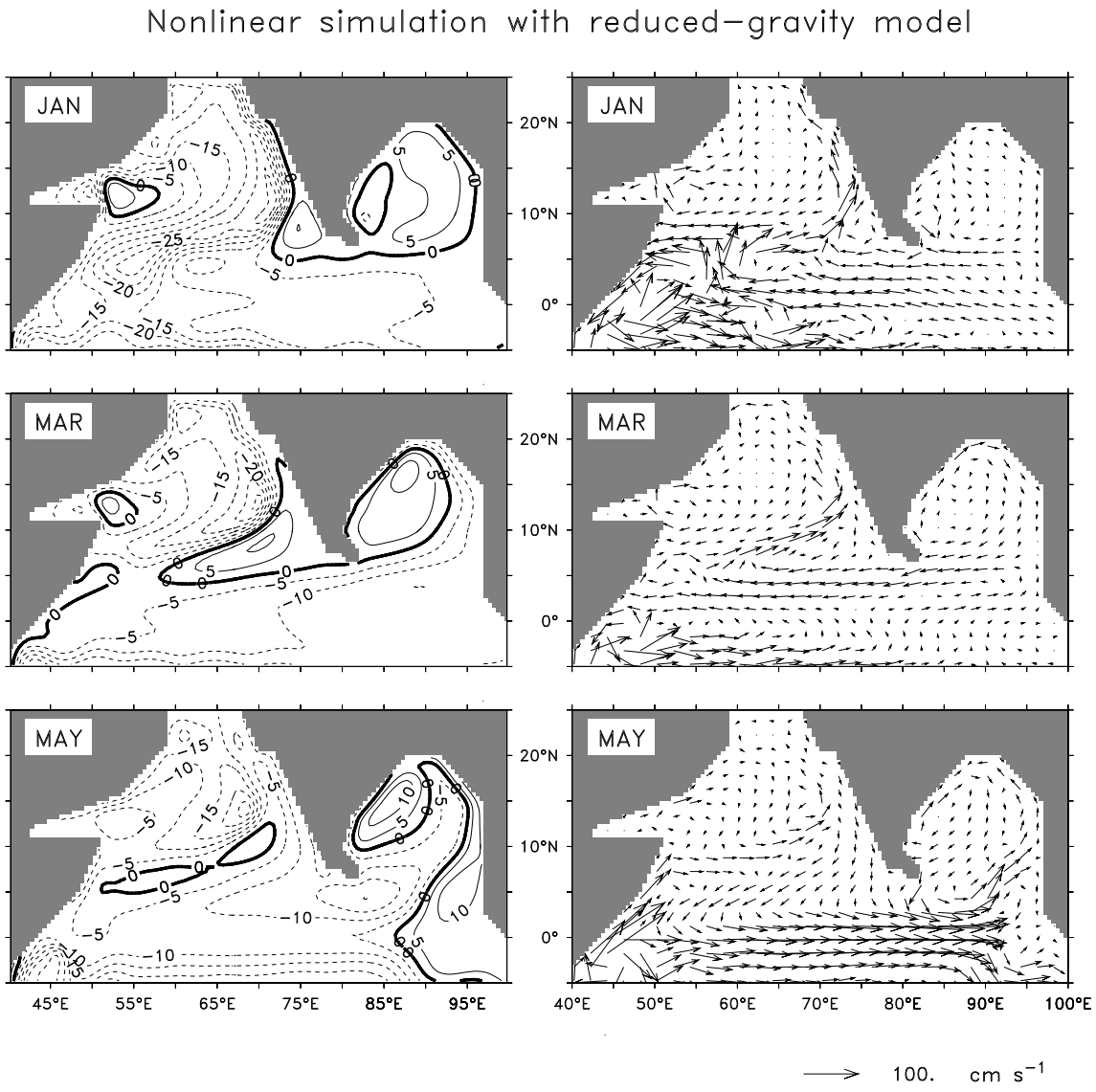

Fig. 16. Sea-level deviation from the initial surface (cm, left panels) and upper-layer velocity (cm s^{-1}, right panels) for the nonlinear simulation. Negative sea level is indicated by dashed contours and the contour interval is 5 cm.

That a linear system is capable of describing the seasonal, open-ocean monsoon currents implies that we can split the solution into components forced by different processes, the sum of these parts then being equal to the whole, the linear solution, which we call the control run. To isolate the effect of individual processes on the monsoon currents, we apply two sets of boundary conditions along continental boundaries (McCreary et al., 1996; Shankar, 1998). One set is the usual no-slip

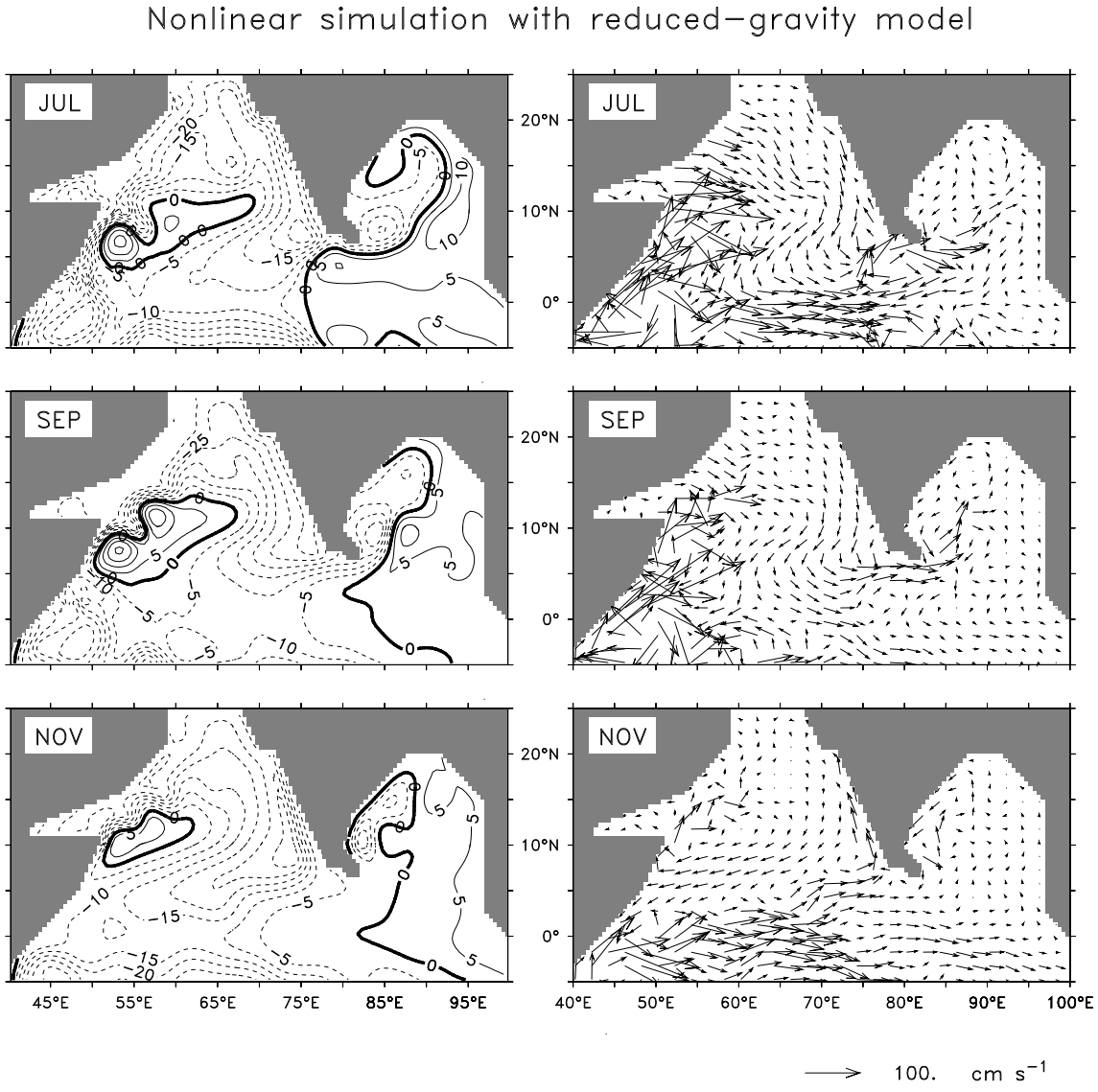

Fig. 16. (continued)

condition

$$u = v = 0. \tag{4a}$$

The other set,

$$\tilde{u} = \mathbf{n} \cdot \mathbf{v} = -\mathbf{n} \cdot \mathbf{k} \times \frac{\tau}{f}, \quad \tilde{v} = \mathbf{k} \times \mathbf{n} \cdot \mathbf{v}, \tag{4b}$$

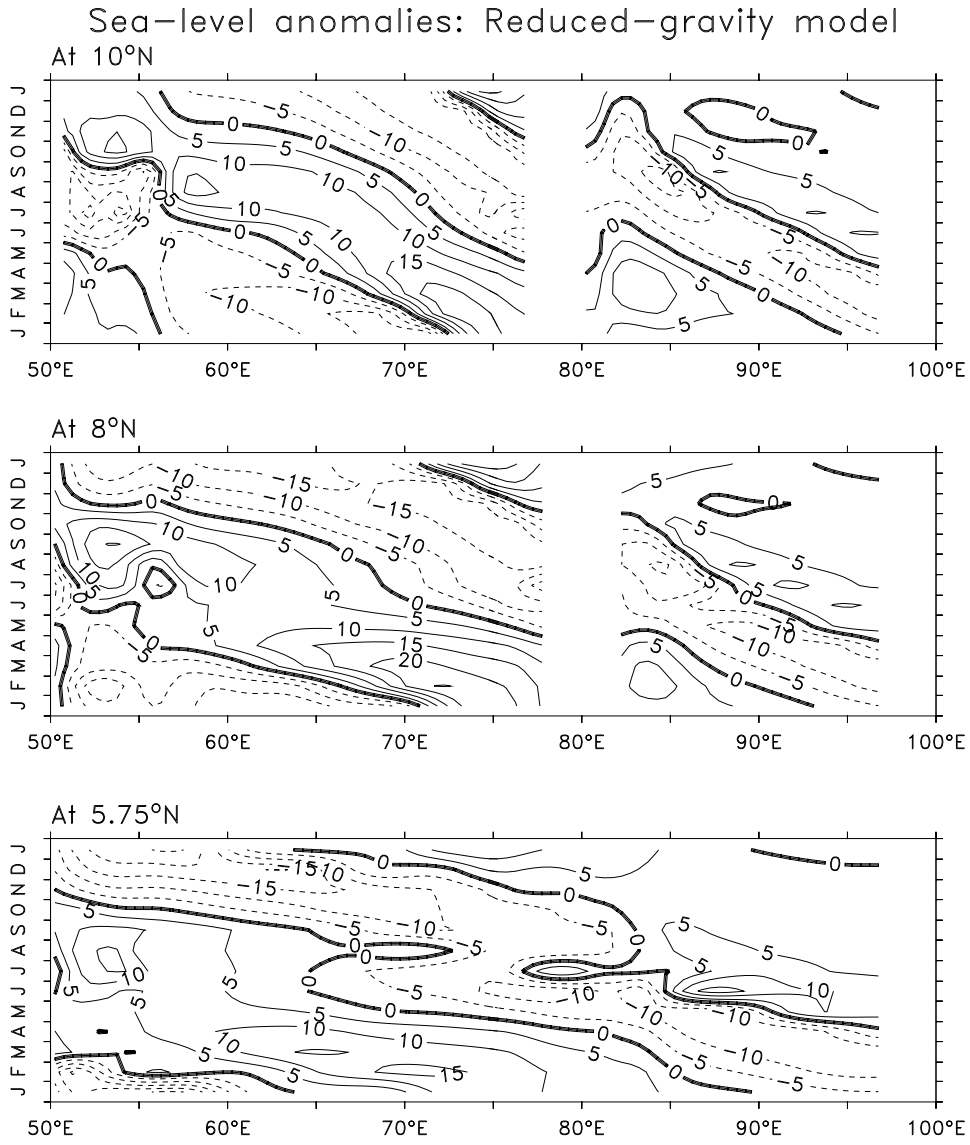

Fig. 17. Longitude-time plots of sea-level anomalies (cm) from the reduced-gravity model (nonlinear simulation) at 10°N (top panel), 8°N (middle panel), and 5.75°N (bottom panel). The annual mean sea level has been removed to obtain the anomalies. Negative sea level is indicated by dashed contours and the contour interval is 5 cm.

is applied to the boundaries of the Bay of Bengal and the Arabian Sea in some of the process solutions. In Eqn. (4b), **k** is a unit vector directed out of the β-plane and **n** is a unit vector normal to the boundary; **n** points out of the Bay of Bengal (inshore) along its eastern and northeastern margins, into the bay (offshore) along its northern and western margins, out of the sea (inshore) along the southern boundaries of India and Sri Lanka and along their west coast, and into the sea (offshore) along the northern and western boundaries of the Arabian Sea; $\mathbf{v} = (\tilde{u}, \tilde{v})$, where $\tilde{u}$ and $\tilde{v}$ are the velocity components normal to and along the boundary; and $\tau = (\tau^x, \tau^y)$ is the

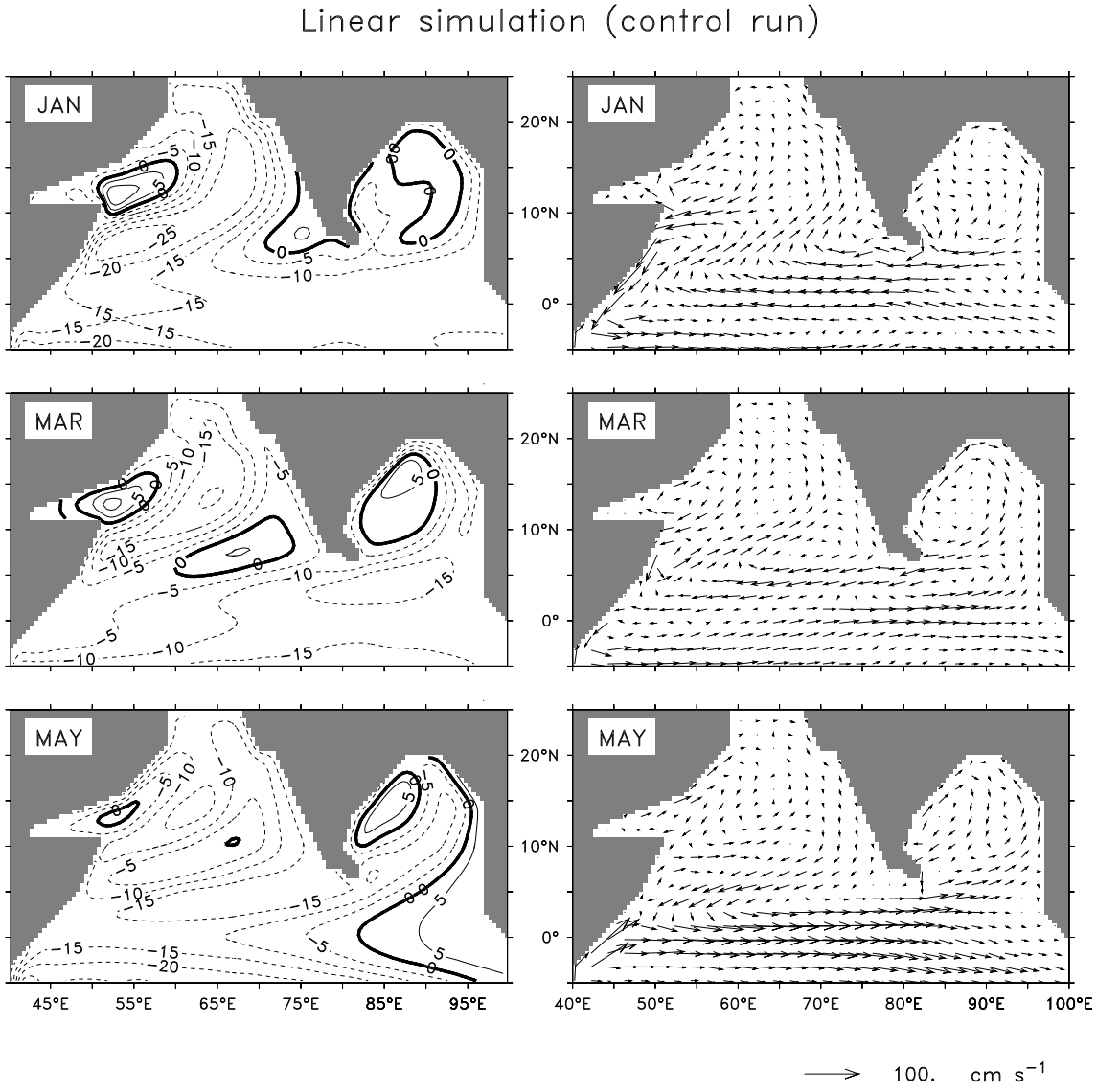

Fig. 18. Sea-level deviation from the initial surface (cm, left panels) and upper-layer velocity (cm s^{-1}, right panels) for the linear simulation. Negative sea level is indicated by dashed contours and the contour interval is 5 cm.

wind stress. Conditions (4b) allow Ekman flows to pass through the boundaries, filtering circulations driven by coastal Ekman pumping out of the solutions; this implies that coastal Kelvin waves are not generated along the coasts where this condition is applied. Condition (4a) is applied at continental boundaries for the control run. The modifications made to obtain the process solutions are described below. The acronyms used for the processes are listed in Table 6.

To isolate the effect of the winds that blow along the eastern and northern boundaries of the Bay of Bengal (process EB here, process RA in McCreary et al. (1996) and Shankar (1998)), we apply conditions (4b) along these coasts, from 2.5°N at the

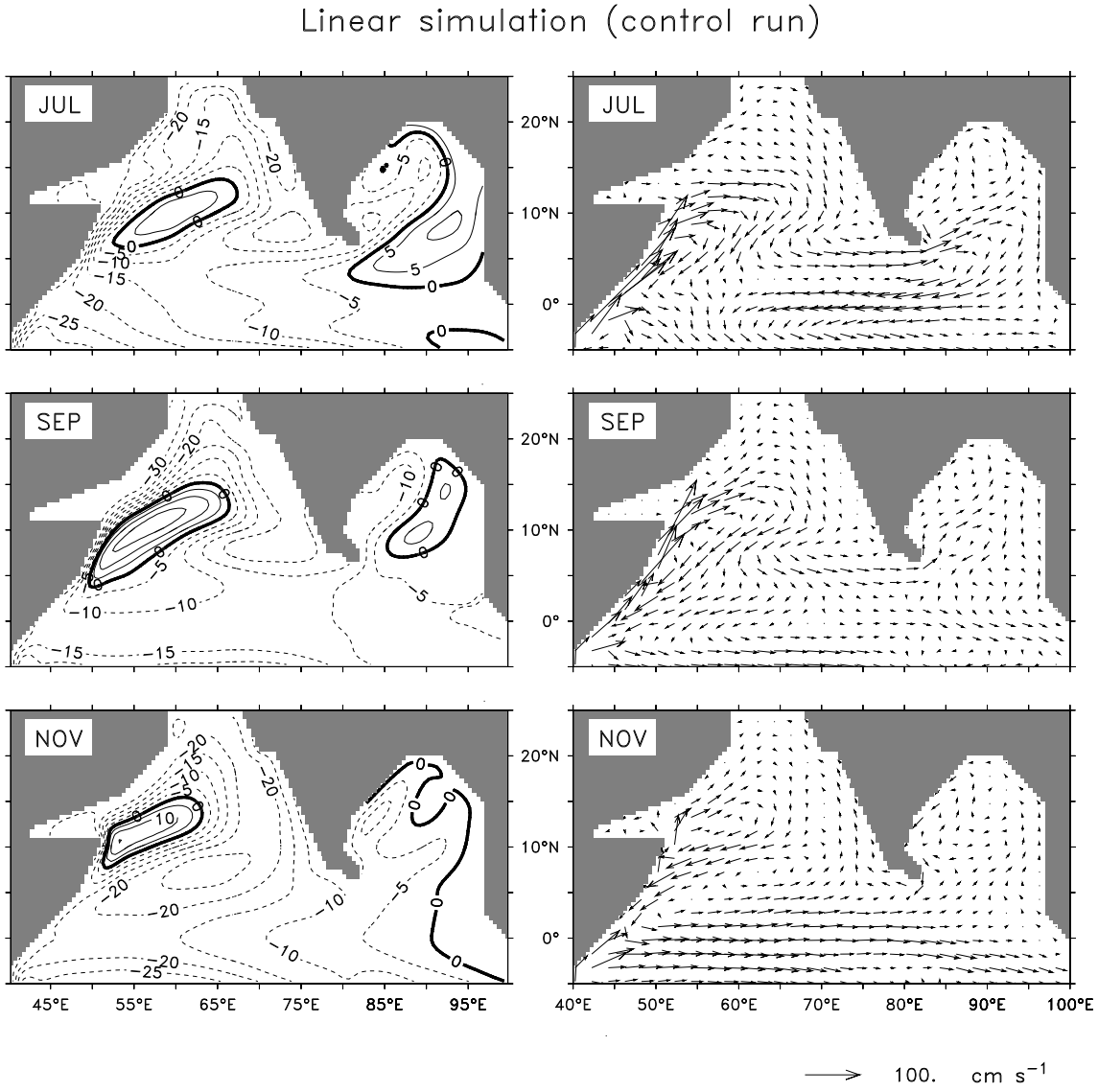

Fig. 18. (continued)

eastern boundary to (87°E, 20°N), thereby eliminating the effect of the alongshore winds there. The difference between the control run and this run gives the process solution forced by EB (not shown). These winds force coastal Kelvin waves, which propagate anticlockwise along the perimeter of the bay, radiating Rossby waves from the eastern boundary in the process. Though the winds in the eastern bay are not significantly weaker than those in the western bay (Fig. 1), the Kelvin waves forced by these winds are weak; it is the alignment of the coast, almost normal to the wind vector, that results in a weak alongshore component, and hence, in a weak response.

Acronym	Process
EB	Effect of winds along the eastern and northern boundaries of the Bay of Bengal (coasts of Thailand, Myanmar, and Bangladesh).
WB	Effect of winds along the western boundary of the Bay of Bengal (east coasts of India and Sri Lanka).
EA	Effect of winds along the eastern boundary of the Arabian Sea (west coasts of Sri Lanka and India).
WA	Effect of winds along the northern and western boundaries of the Arabian Sea (except the coast of Somalia).
SA	Effect of winds along the coast of Somalia.
AW	Effect of alongshore winds, i.e., the winds along the boundaries of the Bay of Bengal and the Arabian Sea (sum of processes EB, WB, EA, WA, and SA).
OP	Other processes — effect of filtering out the alongshore winds (process AW) in the north Indian Ocean. This solution includes Ekman pumping in the interior of the basin and the effect of winds in the equatorial Indian Ocean.

Table 6
Acronyms used for the process solutions.

To isolate the effect of the strong winds that blow along the western boundary of the bay, or the east coast of India and Sri Lanka (process WB here, process LA in McCreary et al. (1996) and Shankar (1998)), we apply conditions (4b) along this coast (from 87°E, 20°N to 82°E, 6.5°N), thereby eliminating the effect of the alongshore winds there. The difference between the control run and this run gives the process solution forced by WB (Fig. 19). The winds along the western boundary of the bay are southwesterly during the summer monsoon and northeasterly during the winter monsoon. The southwest–northeast alignment of the coast makes the wind vector parallel to the coast and these winds generate strong coastal Kelvin waves; the EICC closely follows the wind field. Since the coastal Kelvin waves propagate with the coast on their right in the northern hemisphere, process WB affects only the EICC and has no effect on the circulation elsewhere in the bay. It does, however, have a strong effect on the circulation in the southeastern Arabian Sea (McCreary et al., 1993; Shankar and Shetye, 1997; Shankar, 1998). By itself, it can force the Lakshadweep high and low, the WICC, and the parts of the GWMC and GSMC associated with them. The Lakshadweep high forced by process WB, however, is much stronger than that forced in the control run.

To isolate the effect of the winds that blow along the eastern boundary of the Arabian Sea, or the south and west coasts of Sri Lanka and India (process EA here, process WLA in Shankar (1998)), we apply conditions (4b) along this coast (from 82°E, 6.5°N to 67.5°E, 25°N), thereby eliminating the effect of the alongshore winds there. The difference between the control run and this run gives the process solution forced by EA (Fig. 20). Along this coast, the winds blow equatorward throughout the year, the winds along the west coast of Sri Lanka being the exception; here, in the Gulf of Mannar, the winds are similar to those along the Indian east coast (Shankar, 1998; Luis and Kawamura, 2000). The alongshore winds generate coastal Kelvin waves that propagate poleward along the eastern boundary of the Arabian Sea, radiating westward propagating Rossby waves into the interior in the process. During the summer monsoon, the southwesterlies over the Arabian Sea turn around in the central Arabian Sea to blow from the northwest along the Indian west coast. These winds favour coastal upwelling and are stronger than the equatorward winds during the winter monsoon. The alignment of the coast also ensures that the winds during the winter monsoon generate but a weak coastal Kelvin wave. Therefore, though the winds along the eastern boundary of the Arabian Sea

do not contribute significantly to the Lakshadweep high, they contribute to the Lakshadweep low and force strong upwelling in the eastern and northern Arabian Sea during the summer monsoon. Hence, process EA contributes to the curving flow of the GSMC in the eastern and central Arabian Sea.

The effect of the winds along the northern and western boundaries of the Arabian Sea is evaluated in two parts. First, we consider the effect of winds along the

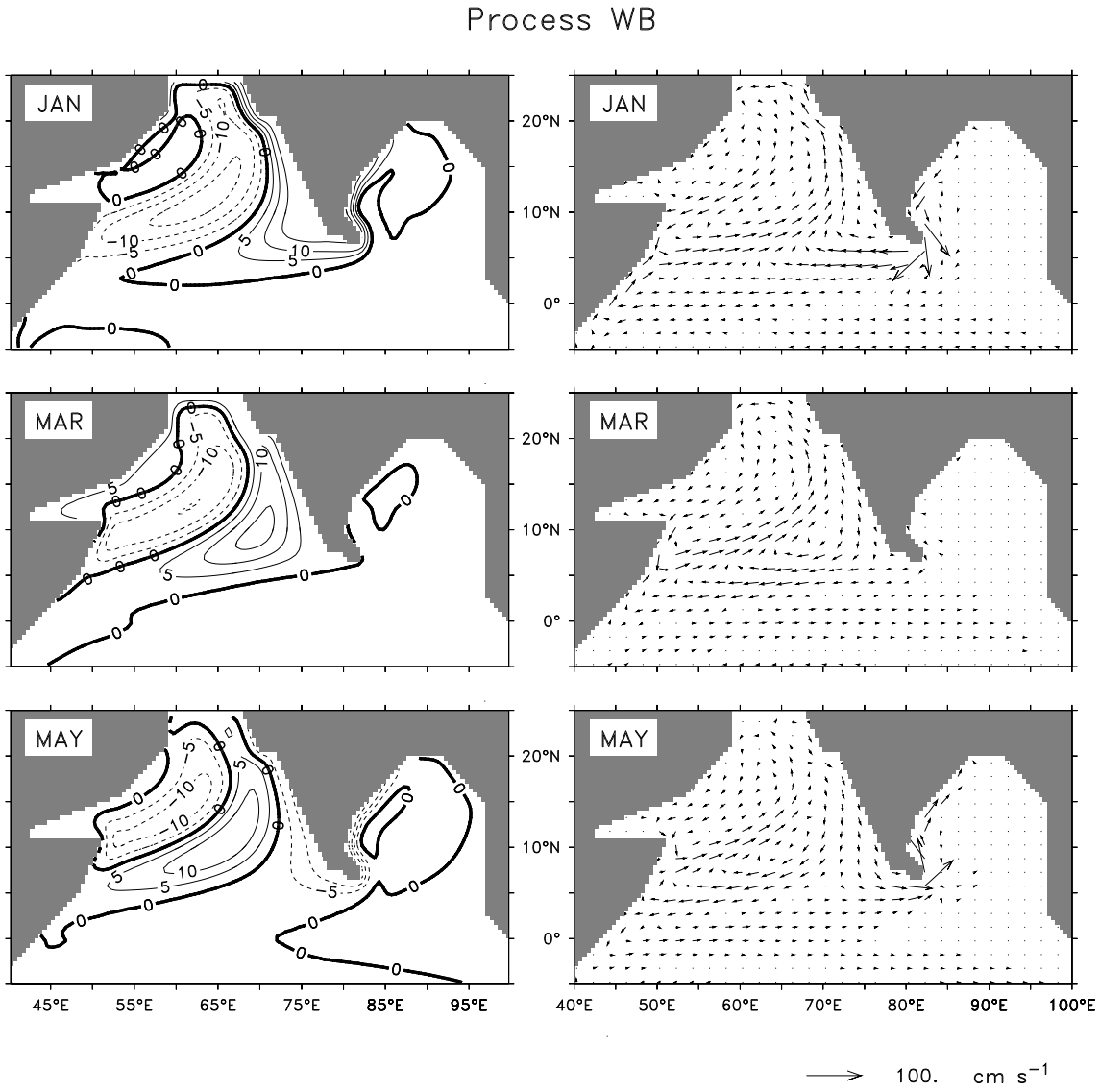

Fig. 19. Effect of winds along the western boundary of the Bay of Bengal (process WB). Sea-level deviation (cm, left panels) and upper-layer velocity (cm s^{-1}, right panels) are shown. Negative sea level is indicated by dashed contours and the contour interval is 5 cm.

boundary from the northeastern corner of the model Arabian Sea (67.5°E, 25°N) to the northern tip of Somalia (process WA), applying conditions (4b) only over this part of the continental boundary; the difference between the control run and this run gives the effect of process WA. Second, we consider the effect of the winds along the coast of Somalia, from the northern tip of Somalia to 2.5°N (process SA), applying conditions (4b) only over this part of the continental boundary; the difference between the control run and this run gives the effect of process SA.

Process WA has only a local effect (Fig. 21). The winds force the local coastal current, with some of the energy propagating equatorward along the coast via coastal

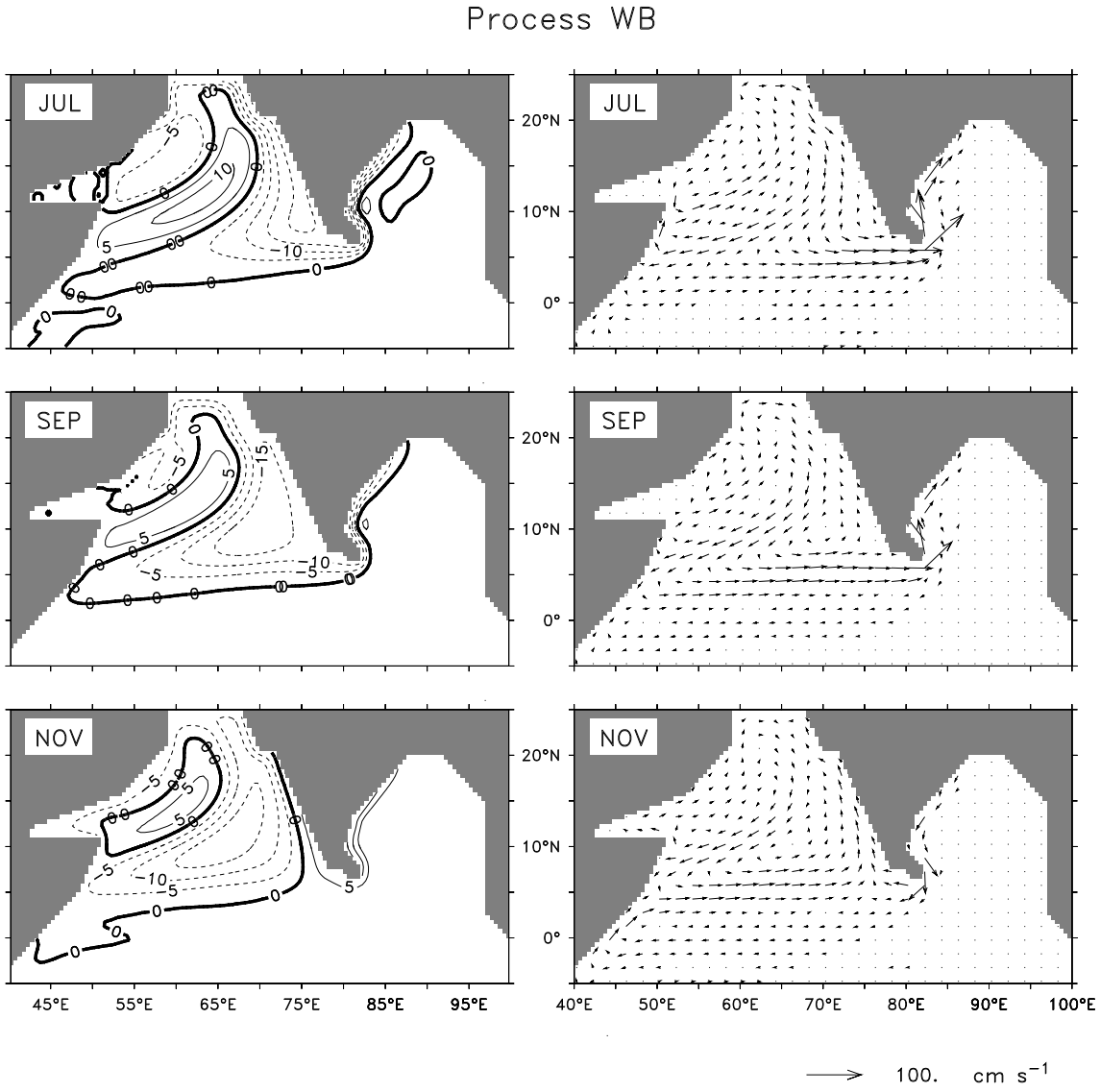

Fig. 19. (continued)

Kelvin waves to the Somali coast.

Process SA is the major forcing mechanism for the strong Somali Current, but its effect is also felt in the equatorial Indian Ocean via Kelvin wave propagation, and in the Bay of Bengal (Fig. 22). The winds off Somalia force strong local upwelling during the summer monsoon, and this signal is carried into the equatorial Indian Ocean, forcing a westward, upwelling-favourable Equatorial Current. This, together with the effect of the Rossby wave reflected from the coast of Sumatra in

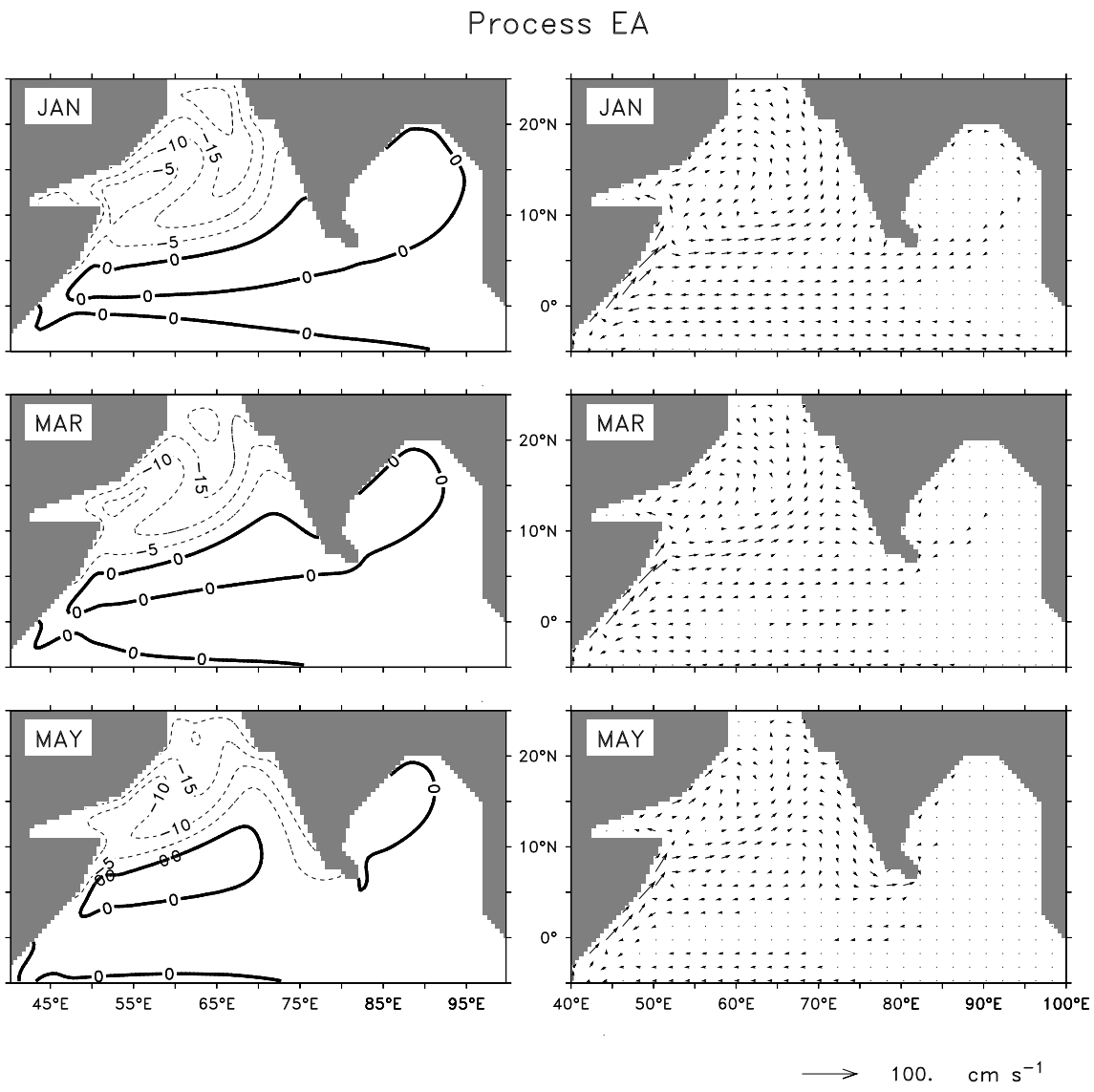

Fig. 20. Effect of winds along the eastern boundary of the Arabian Sea (process EA). Sea-level deviation (cm, left panels) and upper-layer velocity (cm s^{-1}, right panels) are shown. Negative sea level is indicated by dashed contours and the contour interval is 5 cm.

May, ensures a westward Equatorial Current during June–September in the eastern equatorial Indian Ocean and weakens the eastward current in the western equatorial Indian Ocean. This separates the eastward GSMC south of Sri Lanka from the westward flow at the equator.

Applying condition (4b) along all the continental boundaries of the north Indian Ocean (from 2.5°N in the eastern bay to 2.5°N in the western Arabian Sea) eliminates the effect of these coastal winds, filtering out the effect of coastal Kelvin waves generated by them; this leaves the effect of winds in the equatorial Indian Ocean and of Ekman pumping in the interior of the basin (process OP). The differ-

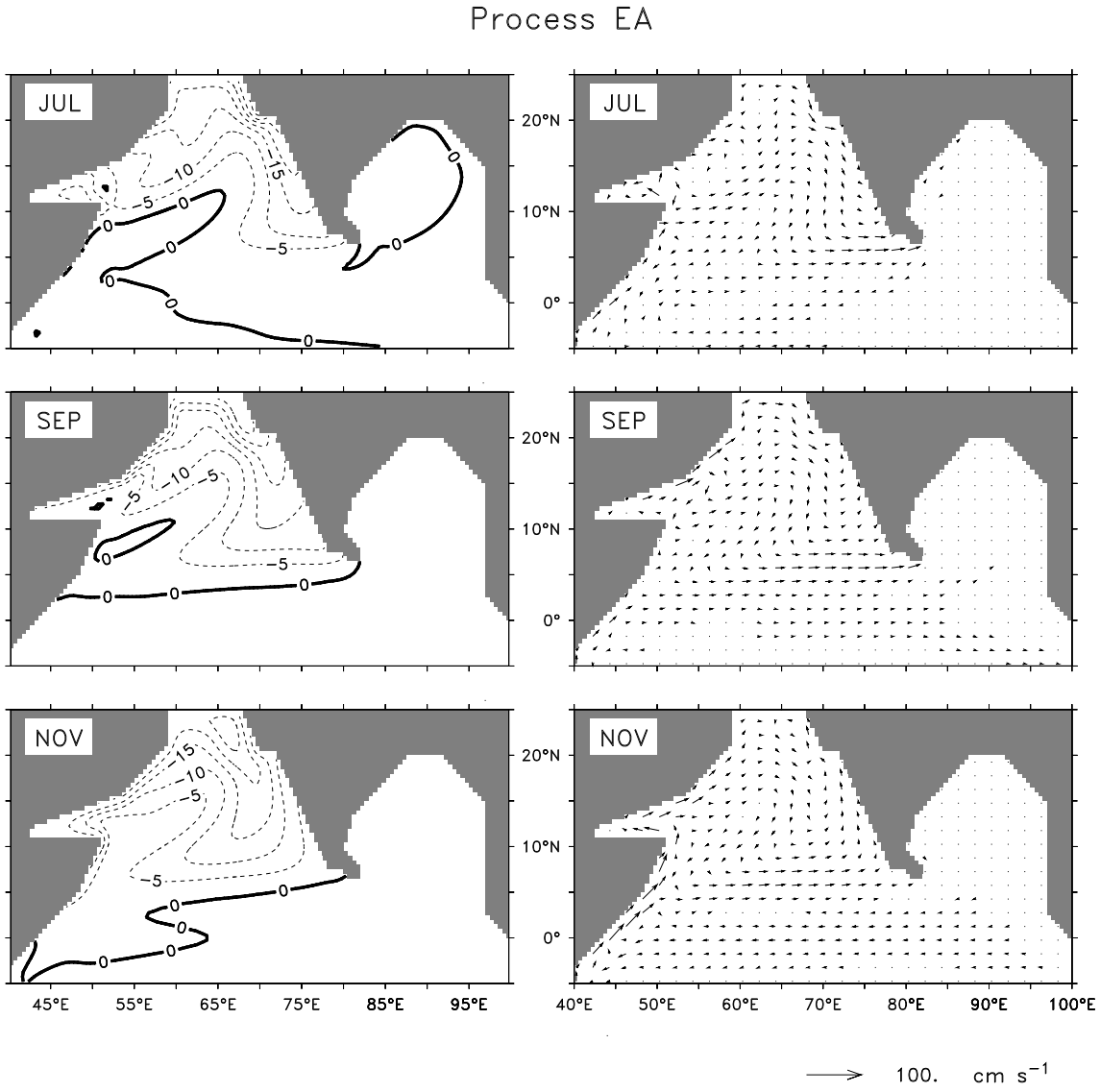

Fig. 20. (continued)

ence between the control run and this run gives the effect of the alongshore winds in the north Indian Ocean (process AW); therefore, process AW is the sum of processes EB, WB, EA, WA, and SA.

Process AW contributes significantly to the circulation (Fig. 23) through the excitation of coastal Kelvin waves and the westward propagating Rossby waves that these Kelvin waves radiate when propagating poleward along an eastern ocean boundary. Most important for the monsoon currents are the winds along the coasts of India and Sri Lanka (processes WB and EA) because it is the forcing by these winds

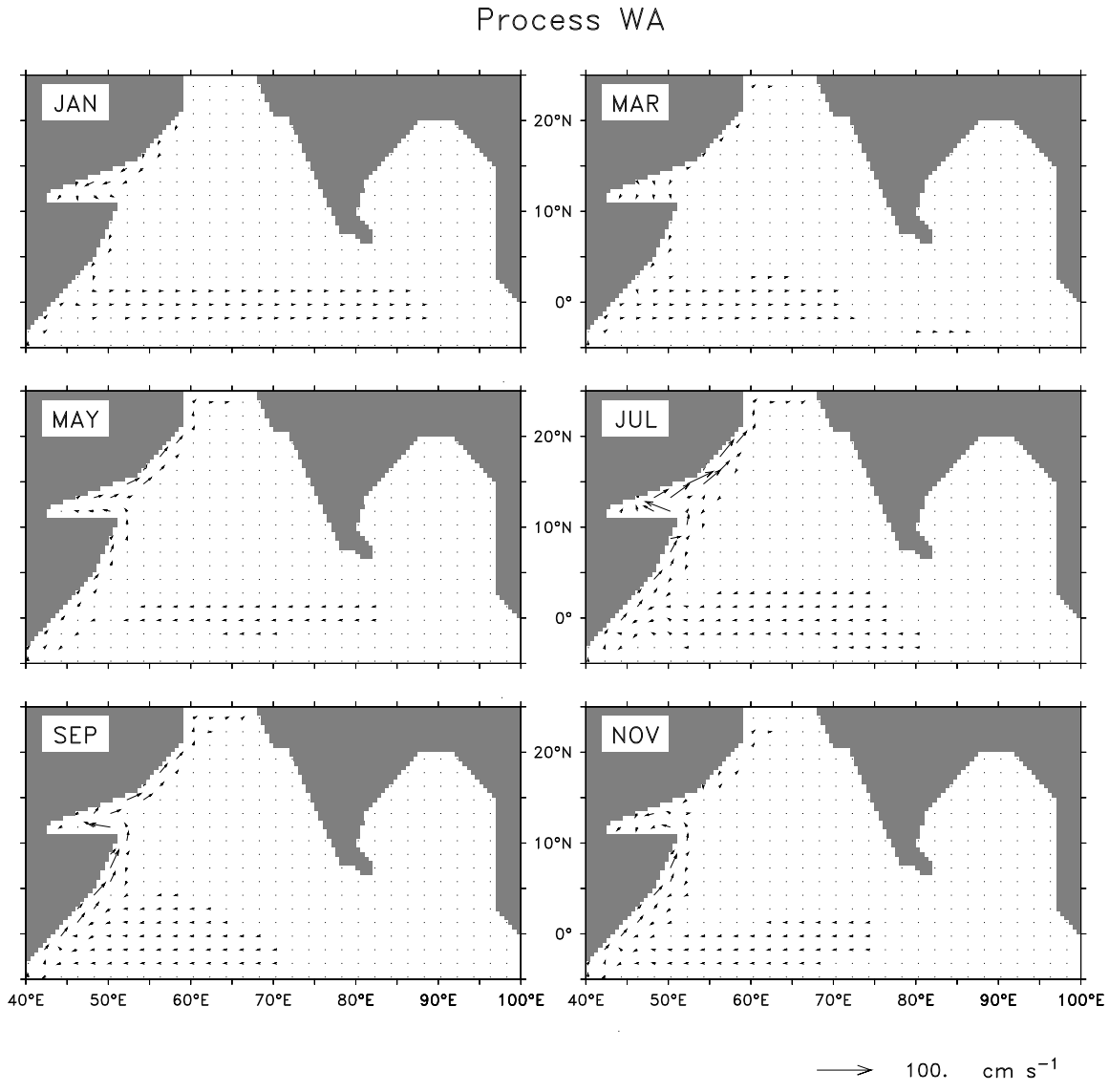

Fig. 21. Effect of winds along the northern and western boundaries of the Arabian Sea, except the Somali coast (process WA). Upper-layer velocity (cm s^{-1}) is shown.

that forces the GSMC and GWMC south of Sri Lanka and in the eastern Arabian Sea, linking the circulation between the two basins. The GWMC and GSMC, however, do not form in the Bay of Bengal in the absence of other processes. The GSMC forced by process AW also flows too far north in the Arabian Sea during the summer monsoon before turning to flow into the WICC, which, in turn, feeds the GSMC around the Lakshadweep low. In the absence of forcing by interior Ekman pumping, the sea-level high in the western Arabian Sea is weak and stretched out, and the GSMC that flows to its south and east does not turn to flow eastward across the southern Arabian Sea.

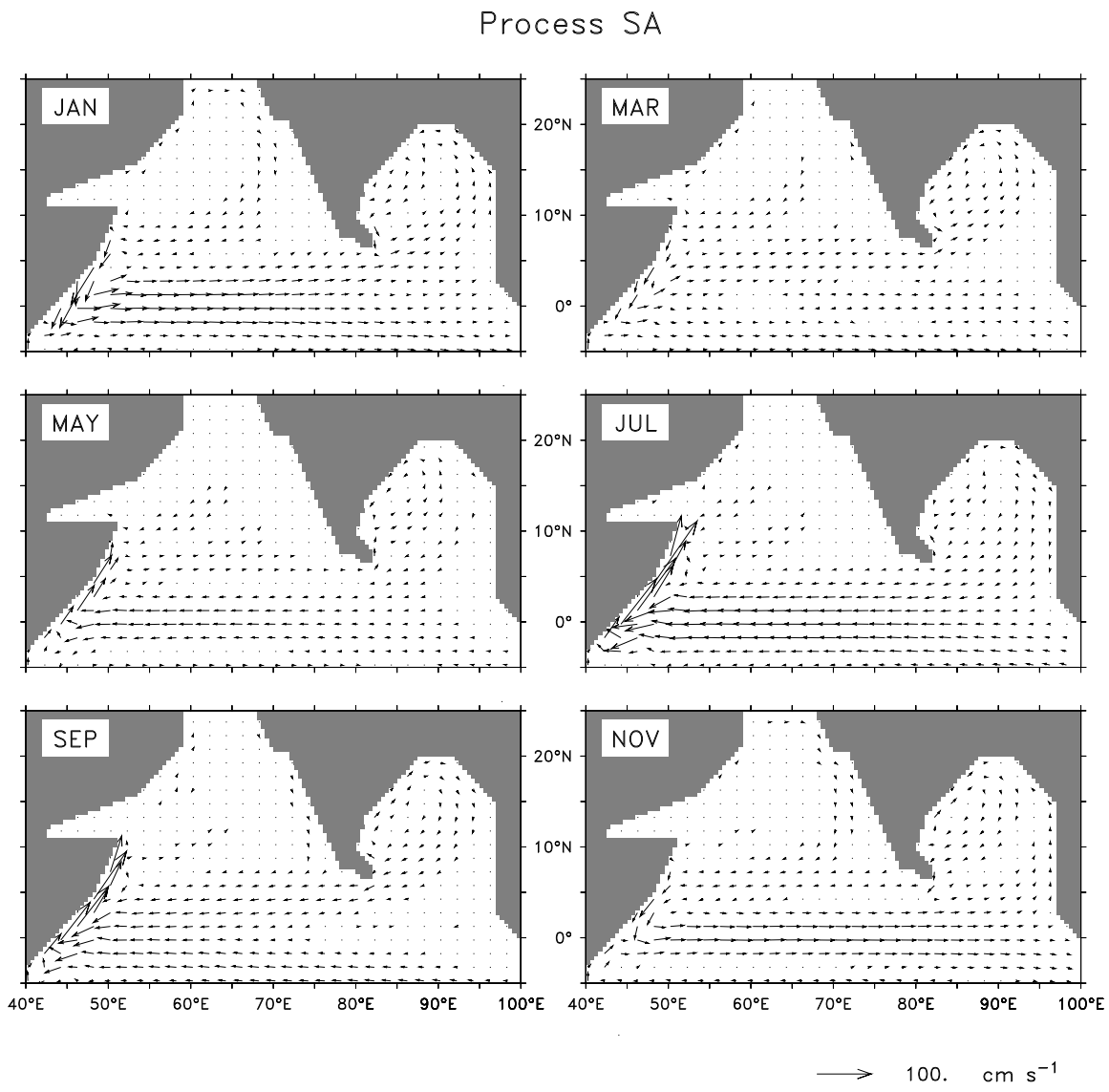

Fig. 22. Effect of winds along the Somali coast (process SA). Upper-layer velocity (cm s^{-1}) is shown.

Process OP, in contrast, is important for the monsoon currents in the Bay of Bengal, where the currents forced by the alongshore winds (process AW) oppose the SMC and WMC, and in the western and central Arabian Sea (Bauer, Hitchcock, and Olson, 1991), where it forces the sea-level highs and the recirculation around them during the summer monsoon (Fig. 24). It is also the only process solution that contains the Ekman drift. The WMC and SMC in the bay are the result of Ekman pumping in the southern bay, especially in the southwest, and of the westward propagating Rossby wave radiated from the eastern boundary owing to the reflection

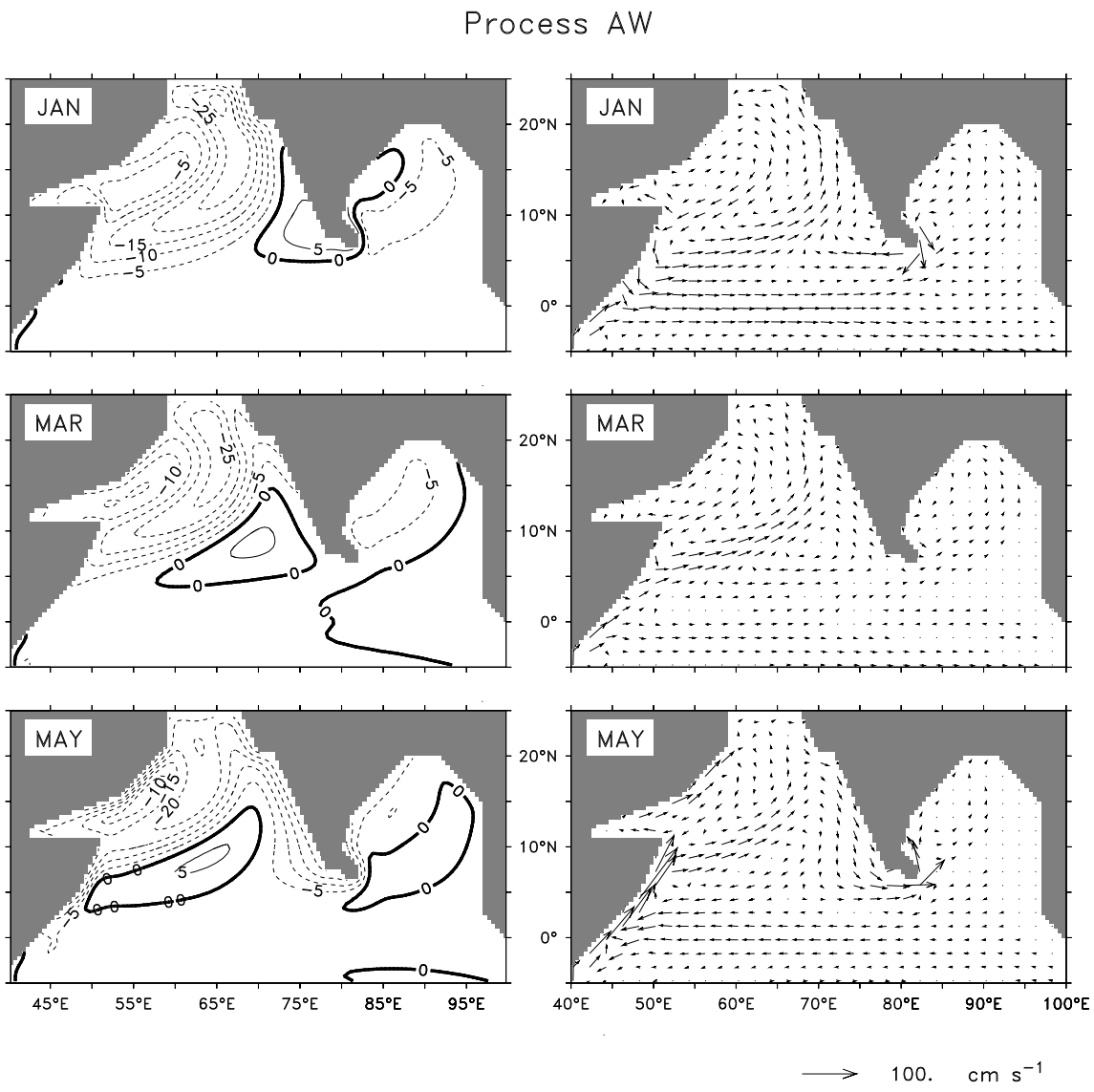

Fig. 23. Effect of alongshore winds in the north Indian Ocean (process AW). Sea-level deviation (cm, left panels) and upper-layer velocity (cm s^{-1}, right panels) are shown. Negative sea level is indicated by dashed contours and the contour interval is 5 cm.

of the equatorial Kelvin wave off Sumatra (Vinayachandran and Yamagata, 1998; Vinayachandran et al., 1999a; McCreary et al., 1993). Not only are these currents forced by Rossby waves, their elimination in the eastern bay and propagation to the west is also due to Rossby waves, but of the opposite sign (Vinayachandran and Yamagata, 1998; Vinayachandran et al., 1999a). During the summer monsoon, the SMC forced by process OP flows westward in the southeastern Arabian Sea, breaking the connection between the SMC in the two basins. This is due to the strong cyclonic Ekman pumping in the vicinity of Sri Lanka (Fig. 25). The continuity of the mature SMC south of Sri Lanka is due to processes WB and EA. This abrupt switch in the mechanisms forcing the SMC south of Sri Lanka (from OP alone to

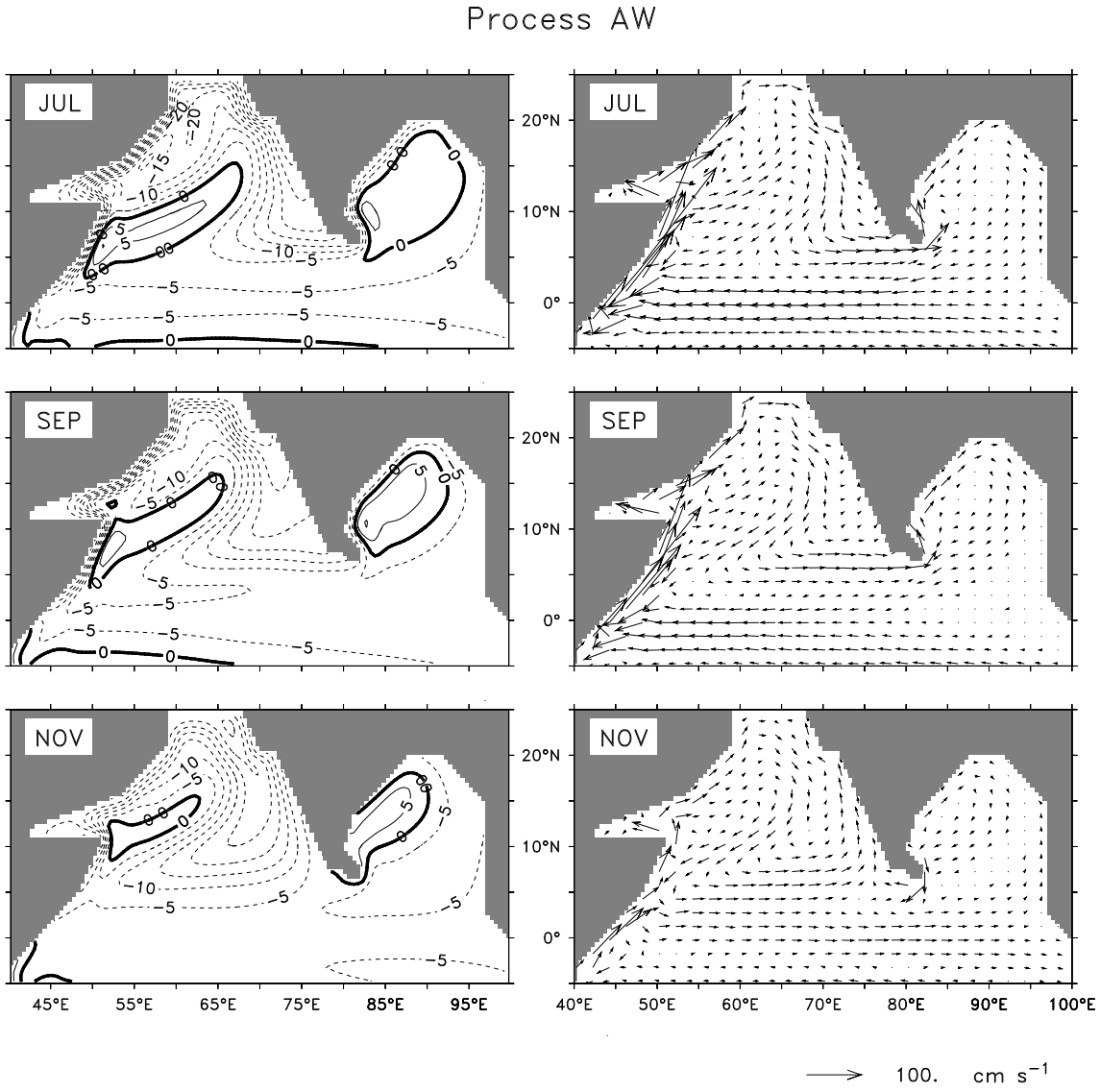

Fig. 23. (continued)

OP, WB, and EA) results in the phase shift there in the sea-level anomalies in both observations (Fig. 6) and model simulations (Fig. 17).

Process OP includes the effect of interior Ekman pumping and that of the winds in the equatorial Indian Ocean. It is difficult to separate these two processes. Applying a damper (McCreary et al., 1996) distorts the reflected Rossby wave; forcing the

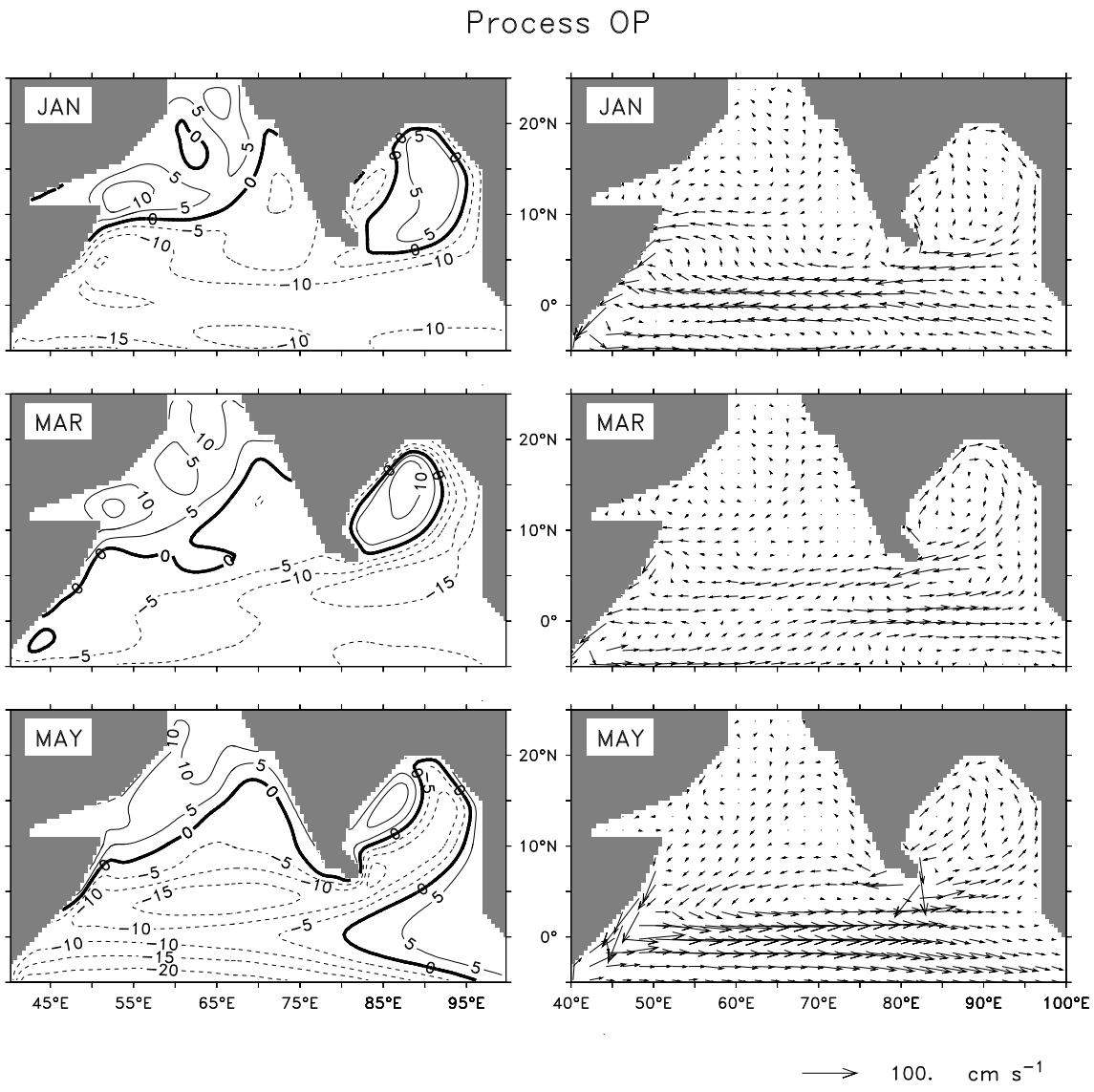

Fig. 24. Effect of filtering out forcing by alongshore winds in the north Indian Ocean (process OP). Sea-level deviation (cm, left panels) and upper-layer velocity (cm s^{-1}, right panels) are shown. Negative sea level is indicated by dashed contours and the contour interval is 5 cm. Process OP includes forcing by interior Ekman pumping and the winds in the equatorial Indian Ocean. It is the only process solution that includes the model Ekman drift.

model with only the equatorial winds (McCreary et al., 1993) distorts the forcing towards the northern and southern edges of the equatorial waveguide because the winds have to be ramped to zero away from it, introducing an additional forcing from the resulting wind-stress curl. Hence, we make no attempt in this paper to break process OP into its constituent processes.

The equatorial winds, however, have been shown to be an important forcing mechanism for the EICC and the WICC (Yu et al., 1991; McCreary et al., 1993, 1996), and the GWMC and GSMC in the Bay of Bengal (McCreary et al., 1993; Vinayachandran et al., 1999a). The forcing from the equatorial Indian Ocean consists of

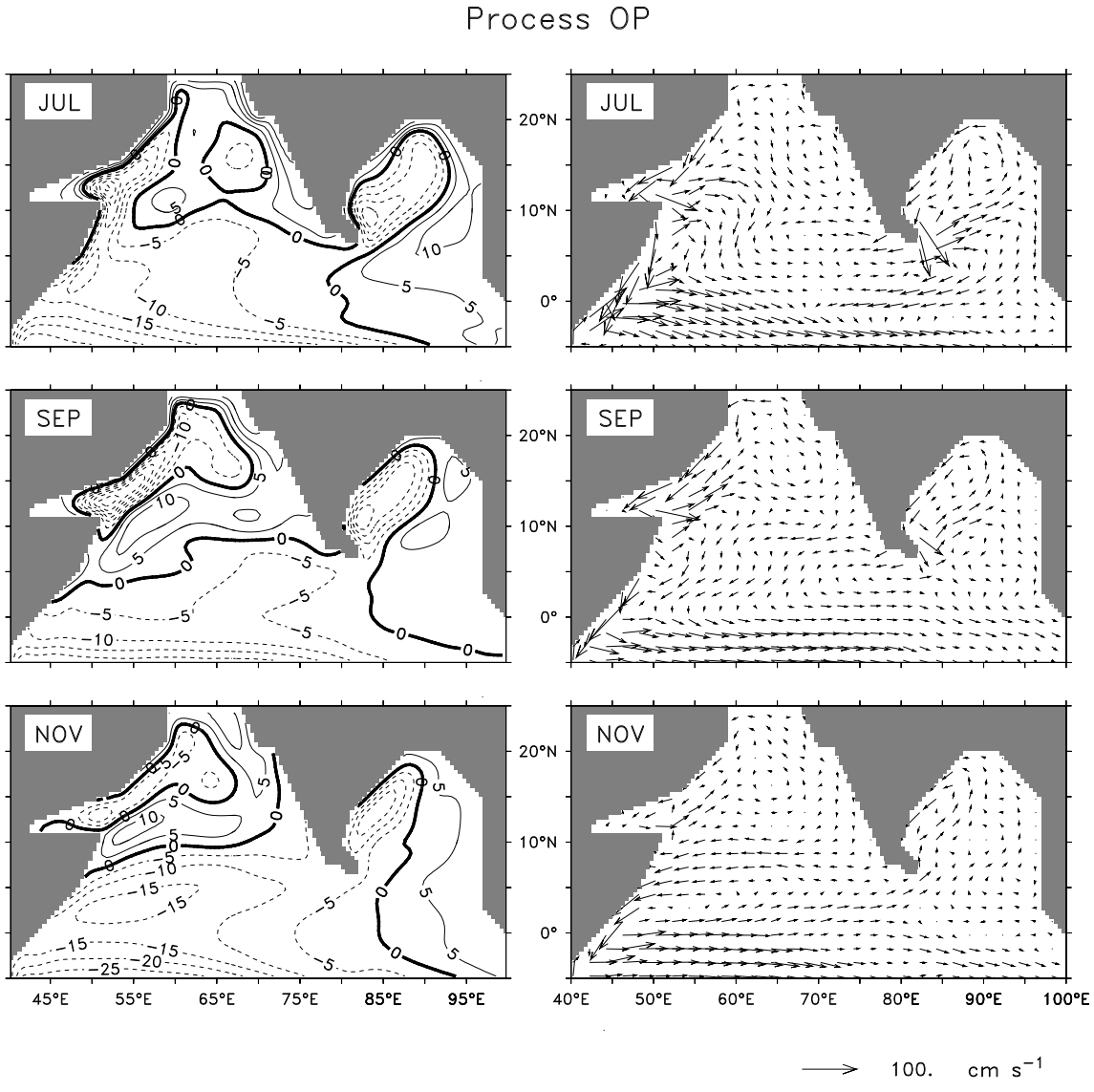

Fig. 24. (continued)

two parts. First, there is the effect of direct forcing, or the generation of equatorial Kelvin and Rossby waves. Second, there is the effect of the reflection of these waves at the eastern and western boundaries. Both processes are crucial to the circulation in the north Indian Ocean, the reflection and resulting resonance being responsible for the large semiannual harmonic at the equator (Figs. 8 and 14) (Jensen, 1993).

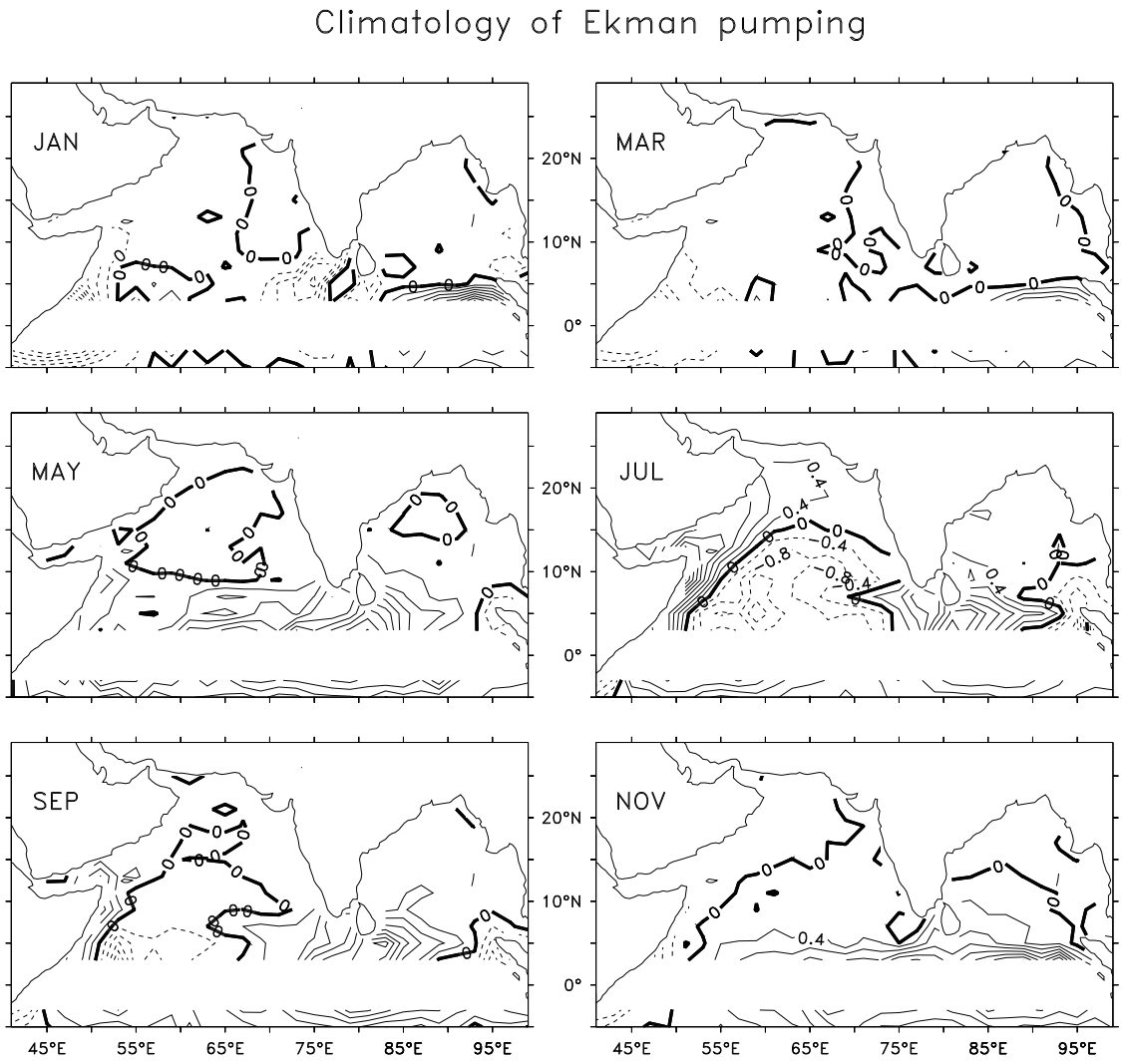

Fig. 25. Ekman pumping (m day^{-1}), derived from the wind-stress climatology of Hellerman and Rosenstein (1983). Negative (downward) Ekman velocity is indicated by dashed contours and the contour interval is 0.4 units.

The numerical experiments described above show that the GSMC and GWMC are complex currents, forced by several processes. The effect of the processes varies in time and space, each process being important at some time and in some part of the north Indian Ocean. The continuity of the GSMC and GWMC across the north Indian Ocean is due to the way these processes interact, connecting the various strands of these currents into a continuous trans-basin current. In spite of this complexity, however, the dynamics of the monsoon currents is explicable by a simple linear theoretical framework, which can be summarized by the "leaky waveguide" (Shetye, 1998; Shankar, 1998) depicted in the schematic in Fig. 26. The framework depicted here invokes the equatorial Kelvin wave (which propagates eastward along the equator with a speed of ~ 2 m s^{-1} and is trapped within $\sim 2.5^\circ$ of the equator), the equatorial Rossby wave (which propagates westward with a speed that decreases with increasing latitude, the speed at the equator being ~ 0.5 m s^{-1}), and the coastal Kelvin wave (which propagates with the coast on its right in the northern hemisphere with a speed of ~ 2 m s^{-1}, and has an offshore *e*-folding length scale of ~ 100 km). These three waves merge the equatorial Indian Ocean, the Bay of Bengal, and the Arabian Sea into a single dynamical entity, the north Indian Ocean, which must be modelled as a whole even to simulate the circulation in its parts.

The process solutions show that the Kelvin waves forced by the winds along the east and west coasts of India and Sri Lanka (processes WB and EA) are crucial for maintaining the continuity of the monsoon currents south of Sri Lanka. The coastal Kelvin waves forced by the winds along the east coast (process WB) bend around Sri Lanka to propagate poleward along the west coast. This is possible because the sum of the *e*-folding scales of the coastal Kelvin waves south of Sri Lanka ($\sim 2.25^\circ$) and the equatorial Kelvin waves ($\sim 2.5^\circ$) is less than the distance between the southern tip of Sri Lanka and the equator ($\sim 6^\circ$), forcing a separation between the equatorial and coastal waveguides. This allows the Kelvin waves from the Bay of Bengal to pass unhindered into the Arabian Sea, making the eastern boundary of the Arabian Sea a continuation of a western boundary, that of the bay. Westward propagating Rossby waves, however, are not restricted to the equatorial waveguide at semiannual and annual periods. Hence, they can interact with the coastal Kelvin

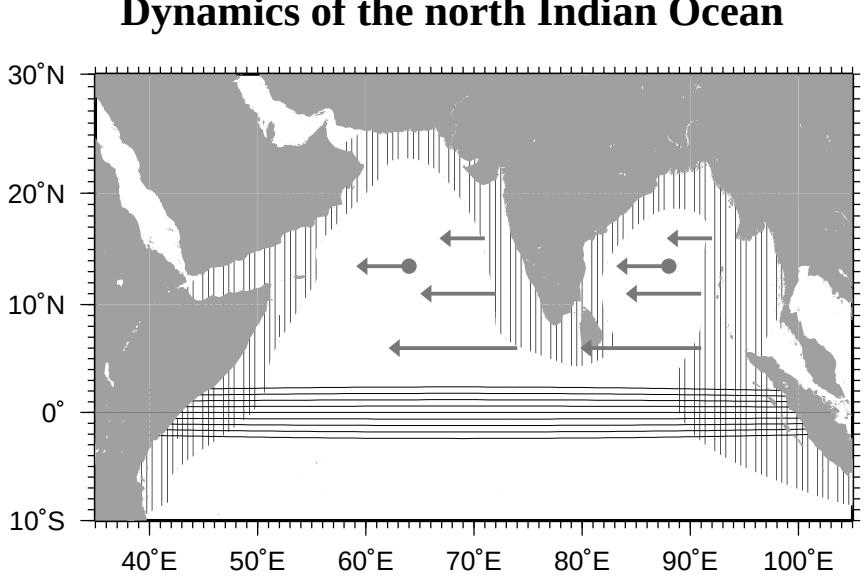

Fig. 26. Schematic illustrating the dynamics of the north Indian Ocean. The linear theoretical framework depicted here invokes the equatorial Kelvin wave, the equatorial Rossby wave, and the coastal Kelvin wave. These three waves merge the equatorial Indian Ocean, the Bay of Bengal, and the Arabian Sea into a single dynamical entity. The horizontal hatching indicates the equatorial waveguide, which extends about 2.5° on either side of the equator; the vertical hatching indicates the coastal waveguide. The coastal Kelvin wave is trapped at the coast poleward of a critical latitude; equatorward of this latitude, westward radiation of energy is possible, and the coastal Kelvin wave is inseparable from the westward propagating Rossby wave. The critical latitudes for Rossby waves at annual (semiannual) period is $\sim 42°$ ($\sim 21°$); hence, annual and semiannual Kelvin waves are inseparable from westward propagating Rossby waves in the north Indian Ocean, and energy leaks at these periods from the eastern boundary into the open ocean (shown by arrows pointing out of the coastal waveguide). Shetye (1998) and Shankar (1998) called this the "leaky waveguide" of the north Indian Ocean. Energy is also generated by Ekman pumping (shown by the closed circles) in the interior of the basin, this signal also propagating westward as Rossby waves.

waves forced by process WB, and influence the monsoon currents south of Sri Lanka.

The two waveguides overlap at the western and eastern boundaries of the equatorial Indian Ocean. Energy from the coastal waveguide leaks into the equatorial waveguide at the western boundary via coastal Kelvin waves, and energy from the equatorial waveguide leaks into the coastal waveguide at the eastern boundary via

the reflection of equatorial Kelvin waves. This reflection at the eastern boundary results in a part of the energy propagating poleward along the eastern boundary of the basin as coastal Kelvin waves (Moore, 1968; Yu et al., 1991). These coastal Kelvin waves are inseparable from the westward propagating Rossby waves almost all over the north Indian Ocean at the semiannual and annual periods (Fig. 26). Energy also leaks out of the coastal waveguide from the eastern boundaries into the interior of the basin via radiation of westward propagating Rossby waves. Westward propagating Rossby waves are also generated in the interior by Ekman pumping.

Thus, complex circulation patterns can be generated even by the simple linear framework described above, which seems to be remarkably good at describing the wind-forced, seasonal circulation in the north Indian Ocean.